$PP + PS = SS$

VLADIMIR GRECHKA and ILYA TSVANKIN
Center for Wave Phenomena, Department of Geophysics,
Colorado School of Mines, Golden, CO 80401-1887, USA

Summary

Converted (PS) waves can provide important information about shear-wave velocity and, in the presence of anisotropy, about the medium parameters responsible for both P- and S-wave propagation. Kinematics and amplitudes of reflected PS-waves, however, possess several undesirable features which preclude application of conventional velocity-analysis methods to mode conversions. Rather than attempting to process converted waves directly, here we propose a method for reconstructing SS-wave reflection traveltimes t_{SS} from PP- and PS-wave data. The key idea of the method is to match the reflection slopes on common-receiver PP- and PS-sections. This matching allows us to find the coordinates of receivers that record PP- and PS-waves reflected at *exactly* the same (albeit unknown) subsurface points. Then, the shear-wave traveltime t_{SS} is found as a simple combination of the PP- and PS-traveltimes. The reconstructed SS-wave moveout can then be processed by velocity-analysis methods designed for pure reflection modes. It should be emphasized that this procedure does not require knowledge of the velocity model and can be applied to data from arbitrary anisotropic, heterogeneous media.

Introduction

For a number of exploration scenarios, PS-waves provide valuable information about the subsurface structure or medium properties that cannot be inferred from conventional PP-wave data. Examples include imaging through gas clouds and estimation of the anisotropic parameters which are not constrained by P-wave data alone. Inversion and processing of PS-waves, however, is seriously impeded by such inherent features of mode conversions as moveout asymmetry, reflection point dispersal and polarity reversal. The most fundamental problem in PS-wave velocity analysis stems from the asymmetry of PS-moveout. In general, the PS-wave reflection traveltime $t_{PS}(\mathbf{x}^{(1)}, \mathbf{x}^{(2)})$ between the source located at $\mathbf{x}^{(1)}$ and the receiver at $\mathbf{x}^{(2)}$ *does not* remain the same if the source and receiver positions are interchanged, i.e., $t_{PS}(\mathbf{x}^{(1)}, \mathbf{x}^{(2)}) \neq t_{PS}(\mathbf{x}^{(2)}, \mathbf{x}^{(1)})$. Therefore, efficient velocity-analysis methods developed for the symmetric moveout of pure modes cannot be applied to PS-waves.

Here, we suggest to abandon the whole concept of PS-wave moveout analysis. Instead, we use PP- and PS-wave reflection traveltimes t_{PP} and t_{PS} to compute the SS-wave traveltimes t_{SS} for the same reflector; this explains the title "$PP+PS = SS$" of our paper. We begin with describing the concept of the method in 2-D and then discuss its extension to 3-D. Finally, numerical and real data examples illustrate application of the method in practice.

Analytic formulation

2-D problem

Suppose PP- and PS-wave reflection data are acquired in the dip direction of the subsurface structure and, if the medium is anisotropic, the vertical incidence plane is a plane of symmetry. This makes the kinematic problem two-dimensional because the reflected rays do not deviate from the incidence plane. For the purpose of theoretical development it is assumed that the P-wave sources and receivers (which record P- and S-arrivals from all sources) are continuously distributed along the line. Another assumption made here is that both PP- and PS-waves are reflected from the *same* interface in the subsurface.

The goal of our procedure is to identify the PP- and PS-rays excited by the same source and reflected at the same point on the interface. Let us examine PP- and PS-wave data near source location $x^{(1)}$ resorted into the common-receiver gathers built for receiver locations $x^{(2)}$ and $x^{(3)}$,

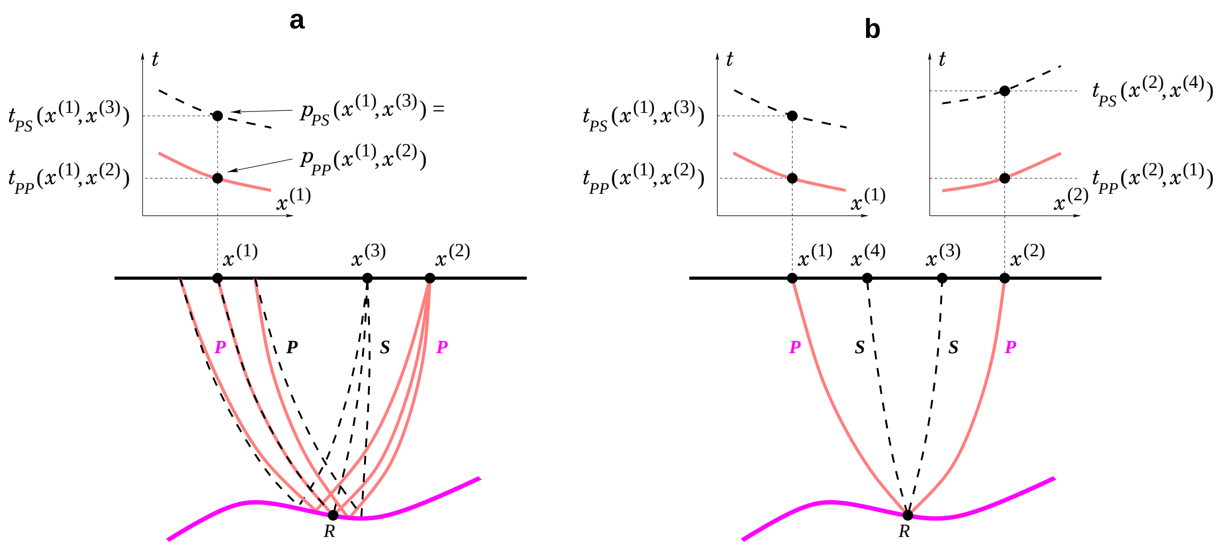

FIG. 1. (a) Matching the reflection slopes $p_{PP}(x^{(1)},x^{(2)})$ and $p_{PS}(x^{(1)},x^{(3)})$ at the source $x^{(1)}$ yields the positions of the receivers $x^{(2)}$ and $x^{(3)}$ which record PP- and PS-waves reflected from the same subsurface point R. (b) Repeating the same procedure for the source at $x^{(2)}$ allows us to find the SS-ray $x^{(3)}Rx^{(4)}$. The reconstructed SS-wave has the same reflection point R as the PP-wave $x^{(1)}Rx^{(2)}$ and the PS-waves $x^{(1)}Rx^{(3)}$ and $x^{(2)}Rx^{(4)}$.

respectively (Figure 1a). Tracking the reflection events on the common-receiver gathers, we can find the traveltimes $t_{PP}(x^{(1)},x^{(2)})$ and $t_{PS}(x^{(1)},x^{(3)})$, along with the local reflection slopes (ray parameters) at the source position $x^{(1)}$:

$$p_{PP}(x^{(1)},x^{(2)}) = \left.\frac{dt_{PP}(x,x^{(2)})}{dx}\right|_{x=x^{(1)}} \quad \text{and} \quad p_{PS}(x^{(1)},x^{(3)}) = \left.\frac{dt_{PS}(x,x^{(3)})}{dx}\right|_{x=x^{(1)}} . \tag{1}$$

For a given P-wave source-receiver pair ($x^{(1)}$, $x^{(2)}$), we are interested in finding a specific receiver location $x^{(3)}$, such that

$$p_{PP}(x^{(1)},x^{(2)}) = p_{PS}(x^{(1)},x^{(3)}) . \tag{2}$$

This equality can be interpreted as an equation for the unknown coordinate $x^{(3)} \equiv x^{(3)}(x^{(1)},x^{(2)})$ that can be found by scanning over receiver locations $x^{(3)}$ along the line. It is not clear in advance whether such a solution exists for any given values of $x^{(1)}$ and $x^{(2)}$, and whether it is unique. If it does not exist, we simply repeat the whole procedure for another pair of ($x^{(1)}$, $x^{(2)}$). If equation (2) has several solutions, as in the case of shear-wave multi-pathing, it is possible to find all of them and reconstruct the multi-valued traveltime t_{SS}.

Suppose that equation (2) has at least one solution $x^{(3)}$. Then rays $x^{(1)}Rx^{(2)}$ and $x^{(1)}Rx^{(3)}$ in Figure 1a have a common segment $x^{(1)}R$ and, therefore, the same reflection point R. Indeed, both rays are excited at the same location $x^{(1)}$ and in the same direction specified by the horizontal slowness $p_{PP}(x^{(1)},x^{(2)}) = p_{PS}(x^{(1)},x^{(3)})$. Therefore, their trajectories have to coincide between the source and the reflection point R, where one of the downgoing waves gets converted into an S-wave. An important point to mention is that both PP-ray $x^{(1)}Rx^{(2)}$ and PS-ray $x^{(1)}Rx^{(3)}$ obey Snell's law at R.

Next, we switch the source and receiver positions by putting the source at $x^{(2)}$ and the receiver at $x^{(1)}$. Repeating the same event-tracking procedure on the common-receiver gathers yields the reflection traveltimes $t_{PP}(x^{(2)},x^{(1)})$ and $t_{PS}(x^{(2)},x^{(4)})$ (Figure 1b), along with the slopes $p_{PP}(x^{(2)},x^{(1)})$ and $p_{PS}(x^{(2)},x^{(4)})$. As before, we find the receiver coordinate $x^{(4)}$ for which the slope $p_{PS}(x^{(2)},x^{(4)})$ of the converted PS-wave on the common-receiver section satisfies the condition

$$p_{PP}(x^{(2)},x^{(1)}) = p_{PS}(x^{(2)},x^{(4)}) . \tag{3}$$

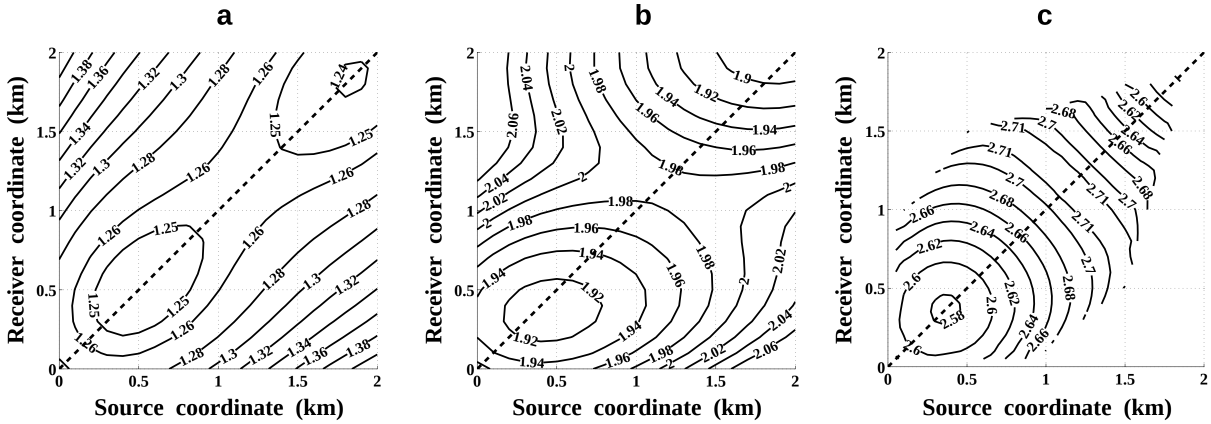

FIG. 2. Traveltimes (in s) of the reflected PP-wave (a), PS-wave (b), and the reconstructed SS-wave (c).

Clearly, ray $x^{(2)}R\,x^{(4)}$ of the converted wave has the same reflection point R (Figure 1b), and the slowness vectors of the downgoing P- and upgoing S-rays for path $x^{(2)}R\,x^{(4)}$ obey Snell's law at R. This implies that the pure shear-wave trajectory $x^{(3)}R\,x^{(4)}$ corresponds to the reflected SS-ray that would be excited at $x^{(3)}$ and recorded at $x^{(4)}$ (or vice versa). As follows from Figure 1b, the reflection traveltime $t_{SS}(x^{(3)}, x^{(4)})$ along this ray is given by

$$t_{SS}(x^{(3)}, x^{(4)}) = t_{PS}(x^{(1)}, x^{(3)}) + t_{PS}(x^{(2)}, x^{(4)}) - t_{PP}(x^{(1)}, x^{(2)})\,. \tag{4}$$

Extension to 3-D

The simplicity of our methodology can be maintained for 3-D multiazimuth data. Let us assume that sources and receivers cover a certain area in the acquisition plane $\mathbf{x} = [x_1, x_2]$. Then, for a given P-wave receiver $\mathbf{x}^{(2)} = [x_1^{(2)}, x_2^{(2)}]$ we build the common-receiver gather (data cube) in the vicinity of the source $\mathbf{x}^{(1)} = [x_1^{(1)}, x_2^{(1)}]$. The PP-wave reflection slope $\mathbf{p}_{PP}\left(\mathbf{x}^{(1)},\, \mathbf{x}^{(2)}\right)$ and the traveltime $t_{PP}\left(\mathbf{x}^{(1)},\, \mathbf{x}^{(2)}\right)$ are found by tracking the event inside the 3-D data volume corresponding to the receiver located at $\mathbf{x}^{(2)}$. The two-component vector $\mathbf{p}_{PP} = [p_{PP,1},\, p_{PP,2}]$, which is equal to the horizontal projection of the traveltime gradient, can be obtained by either fitting a plane to the traveltime surface $t_{PP}\left([x_1,\, x_2],\, \mathbf{x}^{(2)}\right)$ or by numerical differentiation of the obtained traveltime table t_{PP}.

Similarly, we find the PS-wave traveltime $t_{PS}\left(\mathbf{x}^{(1)},\, \mathbf{x}^{(3)}\right)$ and reflection slope $\mathbf{p}_{PS}\left(\mathbf{x}^{(1)},\, \mathbf{x}^{(3)}\right)$ at the source $\mathbf{x}^{(1)}$. If the coordinates $\mathbf{x}^{(3)} = [x_1^{(3)}, x_2^{(3)}]$ of S-wave receiver satisfy the condition

$$p_{PP,\,i}\left(\mathbf{x}^{(1)},\, \mathbf{x}^{(2)}\right) = p_{PS,\,i}\left(\mathbf{x}^{(1)},\, \mathbf{x}^{(3)}\right)\,, \qquad (i = 1, 2), \tag{5}$$

for both horizontal components of the vectors $\mathbf{p}_{PP}$ and $\mathbf{p}_{PS}$, the PP- and PS-rays have the same reflection point R. Next, switching the P-wave source and receiver positions exactly as has been done in 2-D, we find the coordinates $\mathbf{x}^{(4)} = [x_1^{(4)}, x_2^{(4)}]$ of the second S-wave receiver and the corresponding PS-traveltime $t_{PS}\left(\mathbf{x}^{(2)},\, \mathbf{x}^{(4)}\right)$. Finally, the pure shear-wave traveltime $t_{SS}\left(\mathbf{x}^{(3)},\, \mathbf{x}^{(4)}\right)$ is obtained from equation (4).

Synthetic and field-data examples

To demonstrate the performance of the above method, we present a numerical test. Figures 2a and 2b show the PP- and PS-wave reflection traveltimes computed for a layered VTI (transversely isotropic with a vertical axis of symmetry) model with curved interfaces. Note that the traveltimes t_{PS} are asymmetric with respect to zero offset (dashed lines). The reconstructed SS traveltimes (Figure 2c) almost coincide with t_{SS} computed directly by anisotropic ray tracing, with errors up

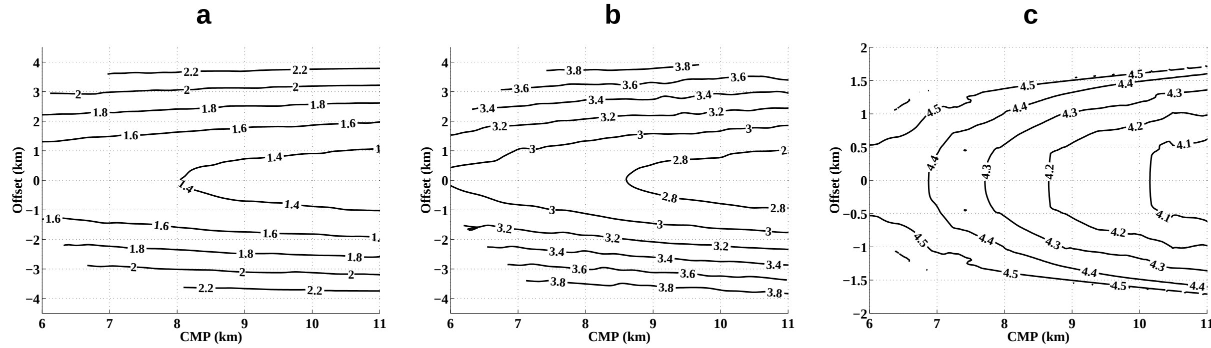

FIG. 3. Raw picked traveltimes (in s) of the PP (a) and PS (b) reflections from an overpressured horizon above the Siri reservoir, and the reconstructed SS traveltimes (c).

to 1.6 ms (0.06%). The small inaccuracies in t_{SS} are caused entirely by the approximations for the reflection slopes and numerical interpolation used to solve equations (2) and (3). As expected, the offsets for the obtained SS reflections Figure 2c are smaller than those for the input PP- and PS-waves.

Our methodology was also applied to PP- and PS-wave reflection data acquired above the Lower Tertiary Siri reservoir in the North Sea. Figure 3 displays the recorded PP and PS data and the reconstructed SS traveltimes for one of the horizons above the Siri reservoir. Joint inversion of the PP and SS data made it possible to build a layered VTI velocity model of the subsurface (Grechka et al., 2001c) and generate high-quality anisotropic PS-wave images of the reservoir (Hansen et al., 2001).

Conclusions

We have suggested a methodology for reconstructing the traveltimes of pure SS-wave reflections from PP- and PS-wave traveltime data that can be used for arbitrary anisotropic, heterogeneous media. The main features of the method are summarized below.

- The method is not model-dependent, and no information about the velocity field or anisotropic parameters is required to obtain the SS-wave traveltimes.
- If the input PP and PS arrivals correspond to the same reflector, the method produces the *exact* traveltimes t_{SS}. Inaccuracy in picking the PP- and PS-wave traveltimes and reflection slopes is the only source of errors in t_{SS}.
- The estimates of traveltimes and reflection slopes are *local*, which makes moveout asymmetry and reflection-point dispersal of PS-waves irrelevant.
- Another consequence of the local nature of this procedure is that the portion of PS data in the vicinity of the polarity reversal (where the PS amplitudes are small) can be muted out without compromising the quality of t_{SS} estimates.
- Once the traveltimes t_{SS} are found, they can be processed by means of any velocity-analysis technique developed for pure modes. Note, however, that our method is not designed to recover the correct amplitudes of SS-reflections.

The reconstructed SS-wave traveltimes are especially attractive for anisotropic stacking-velocity tomography because they provide information complimentary to that in PP-wave data. The anisotropic parameter-estimation methodology developed for PP-waves (Grechka et al., 2001a,b) can be extended in a straightforward way to the combination of PP- and SS-data, as demonstrated by Grechka et al. (2001c).

References

Grechka, V., Pech, A., and Tsvankin, I., 2001a, Inversion of P-wave data in laterally heterogeneous VTI media. Part I: Plane dipping interfaces: 63rd Conference of EAGE, Amsterdam, this volume.

Grechka, V., Pech, A., and Tsvankin, I., 2001b, Inversion of P-wave data in laterally heterogeneous VTI media. Part II: Irregular interfaces: 63rd Conference of EAGE, Amsterdam, this volume.

Grechka, V., Tsvankin, I., Bakulin, A., and Hansen, J.O., 2001c, Joint inversion of PP and PS reflection data for layered VTI media: A North Sea case study: 63rd Conference of EAGE, Amsterdam, this volume.

Hansen, J.O., and Bakulin, A., 2001, The effect of seismic anisotropy on multicomponent imaging and AVO: 63rd Conference of EAGE, Amsterdam, this volume.